

# Estimating Turbulence Kinetic Energy Dissipation Rates in Atmospheric Flows: A Priori Study



Emmanuel O. Akinlabi, Marta Waclawczyk, Juan Pedro Mellado and Szymon P. Malinowski

**Abstract** In this work, Direct Numerical Simulations (DNS) of atmospheric convective boundary layer flow is used to test various approaches to estimate turbulence kinetic energy dissipation rate (EDR)  $\epsilon$  from one-dimensional (1D) velocity signals. Results of these estimates are compared with “true” DNS values of  $\epsilon$ . We focus on methods of EDR retrievals proposed recently in Waclawczyk et al. *Atmos. Meas. Tech.* **10**, 2017. We test these methods and show that they provide a valuable complement to standard approaches. Another goal is to investigate how the presence of anisotropy due to buoyancy affect the various retrieval techniques of  $\epsilon$ .

## 1 Introduction

Mean EDR is an important quantity that characterizes small scales of turbulence. At the same time our information on such scales in atmospheric turbulence is scarce. Due to finite sampling frequency and measurement errors, velocity time series from airborne measurements are characterized by effective spectral cut-off's [2]. Additionally, atmospheric flows in clouds and boundary layers are mostly inhomogeneous and buoyant and may also include the co-existence of laminar and turbulent regions called external intermittency. Hence, results of EDR retrieval are subject to errors.

EDR retrieval methods that are commonly used in the analysis of low and moderate resolution velocity time series are based on the inertial range arguments that follow from the Kolmogorov's hypotheses (K41) [3]. In case the signals are fully resolved, the variance of velocity fluctuation gradients can be calculated to estimate  $\epsilon$ . Alternatively, Sreenivasan et al. [7] proposed to use the zero-crossing approach, which requires counting the number of times per unit length the velocity signal crosses the zero threshold, denoted by  $N_l$ .

---

E. O. Akinlabi (✉) · M. Waclawczyk · S. P. Malinowski  
Faculty of Physics, Institute of Geophysics, University of Warsaw, Warsaw, Poland  
e-mail: [Emmanuel.Akinlabi@fuw.edu.pl](mailto:Emmanuel.Akinlabi@fuw.edu.pl)

J. P. Mellado  
Max-Planck Institute for Meteorology, Hamburg, Germany

Since  $N_l$  in signals with spectral cut-off are much smaller than in fully resolved velocity signals, two possible modifications to the zero-crossing method were proposed in [8]. First of them was based on the successive filtering of the velocity signal. The second approach was an analytical model to resolve the missing part of the spectrum by calculating a correcting factor to  $N_l$  so that the actual relation between  $\epsilon$  and  $N_l$  can be used. These approaches were validated on the data obtained during the Physics of Stratocumulus Top (POST) research campaign [4] in [8] and on DNS data of stratocumulus cloud-top in [1].

In this work we consider yet another flow case, the atmospheric convective boundary layer flow. The motivation is to investigate how the presence of anisotropy due to buoyancy affect the various retrieval techniques of  $\epsilon$ .

## 2 EDR Retrieval Methods

The EDR is defined as  $\epsilon = 2\langle s_{ij}s_{ij} \rangle$  where  $\nu$  is the kinematic viscosity and  $s_{ij} = 1/2(u'_{i,j} + u'_{j,i})$ ,  $u'_i$  denotes the  $i$ th component of velocity fluctuation vector. This exact definition cannot be used to estimate  $\epsilon$  in case only 1D intersections of turbulent velocity field are available from experiments and/or the measured velocity time series have spectral cut-offs due to e.g. finite sampling frequency of a sensor.

Under the local isotropy assumption [3] a direct relation between EDR and the longitudinal, or transverse Taylor microscale ( $\lambda_l$  or  $\lambda_n$ ) can be used to estimate  $\epsilon$  from a single, e.g. longitudinal, fluctuating velocity component  $u'_l$

$$\epsilon_\lambda = 30\nu\langle u_l'^2 \rangle / \lambda_l^2, \text{ where } \lambda_l = [2\langle u_l'^2 \rangle \langle (\partial u_l' / \partial x)^2 \rangle^{-1}]^{1/2} \text{ and } \lambda_n = \lambda_l / \sqrt{2}.$$

Another method for calculating EDR was proposed in [7] and is based on the number of signals' zero-crossings per unit length  $N_l$ . The zero-crossing, Liepmann scale was defined as  $\Lambda = 1/\pi N_l$  [7], and it was assumed that  $\Lambda/\lambda_n \approx 1$ . This allows to estimate the EDR from  $\epsilon_{SR} = 15\pi^2\nu\langle u_l'^2 \rangle N_l^2$ .

In case only restricted range of wavenumbers is available from experiment the Kolmogorov's second similarity hypothesis must be used [3] to approximate  $\epsilon$ . Under the local isotropy assumption, the longitudinal and transverse energy spectra  $E_{11}(k_1)$  and  $E_{22}(k_1)$  ( $k_1$  is the wavenumber) follow the  $-5/3$  law in the inertial range

$$E_{11}(k_1) = \alpha \epsilon_{PS}^{2/3} k_1^{-5/3} \quad E_{22}(k_1) = \alpha' \epsilon_{PS}^{2/3} k_1^{-5/3} \quad (1)$$

where  $\alpha \approx 0.49$ ,  $\alpha' \approx 0.65$  and  $\epsilon_{PS}$  should approximate the EDR  $\epsilon$ . Alternatively, the profiles of the second and third order longitudinal structure functions  $D_2(r)$  and  $D_3(r)$  can be used, where  $D_n = \langle (u'_l(x+r, t) - u'_l(x, t))^n \rangle$  and  $u'_l$  is the longitudinal component of velocity fluctuation. In the inertial subrange [3]

$$D_2(r) = C_2 \epsilon_{D_2}^{2/3} r^{2/3}, \quad D_3(r) = -\frac{4}{5} \epsilon_{D_3} r, \quad (2)$$

where  $\epsilon_{D_2}$  and  $\epsilon_{D_3}$  are approximations of  $\epsilon$ .

In [8] two alternative methods to estimate  $\epsilon$  from the number of crossings based on a restricted range of  $k$ -values were proposed. The motivation was to possibly increase robustness of  $\epsilon$  retrieval using different statistics. The first method was based on the successive filtering of the signal. The EDR was estimated from

$$\pi^2(\langle u_1'^2 \rangle N_1^2 - \langle u_i'^2 \rangle N_i^2) = 3\alpha \epsilon_{\text{NC}}^{2/3} \left( k_1^{4/3} - k_i^{4/3} \right), \tag{3}$$

where  $\langle u_i'^2 \rangle$  is the variance and  $N_i$  is the number of crossings per unit length of a signal filtered with a cut off wave-number  $k_i$  inside the inertial range. Filtering the signal with a series of cut-off wave-number  $k_i$ , allows to estimate  $\epsilon_{\text{NC}}$  from (3).

The second method is based on recovering the missing (unresolved) part of the spectrum. It requires assumption about the form of the spectrum in the inertial and dissipative range. The number of crossings per unit length  $N_{\text{cut}}$  is calculated from the measured signal  $u'_{\text{cut}}$ , where the fine-scale fluctuations have the highest wave number  $k_{\text{cut}}$ , which may be placed in the inertial or the dissipative range. It was proposed in [8] to estimate EDR from

$$\epsilon_{\text{NCR}} = 15\pi^2 \nu \langle u_{\text{cut}}'^2 \rangle N_{\text{cut}}^2 C_{\mathcal{F}}, \tag{4}$$

where  $C_{\mathcal{F}}$  is a correcting factor described by the formula

$$C_{\mathcal{F}} = 1 + \frac{\int_{k_{\text{cut}}\beta\eta}^{\infty} \xi_1^2 \int_{k_1}^{\infty} \xi^{-8/3} f_{\eta}(\xi) \left( 1 - \frac{\xi_1^2}{\xi^2} \right) d\xi d\xi_1}{\int_0^{k_{\text{cut}}\beta\eta} \xi_1^2 \int_{\xi_1}^{\infty} \xi^{-8/3} f_{\eta}(\xi) \left( 1 - \frac{\xi_1^2}{\xi^2} \right) d\xi d\xi_1}, \tag{5}$$

where  $\eta = (\nu^3/\epsilon)^{1/4}$  is the Kolmogorov’s microscale and  $f_{\eta}$  is a prescribed form of the spectrum in the dissipative range. We compared different forms of  $f_{\eta}$  in [1] and found that the best results are obtained with the Pope’s model spectrum [6].

In order to calculate  $C_{\mathcal{F}}$  from (5) a value of  $\eta$  should first be specified, hence, an iterative procedure was proposed in [8]. It starts with an initial guess of the TKE dissipation rate,  $\epsilon^0$ . With this, the corresponding value of the Kolmogorov length  $\eta_0$  is calculated and introduced into (5) for  $C_{\mathcal{F}}$ . The TKE dissipation rate after the first iteration,  $\epsilon^1$  is found from (4). The procedure can be repeated and after several iterations it converges to the final value of  $\epsilon_{\text{NCR}}$  which should approximate  $\epsilon$  with an error defined by a prescribed form  $\Delta\eta = |\eta^{n+1} - \eta^n| < d_{\eta}$ .

### 3 Description of Free Convective Boundary Layer Simulation

Different EDR retrieval techniques are tested on DNS data of a dry, shear-free convective boundary layer CBL that grows into a linearly stratified atmosphere (cf. Fig. 1). The flow is driven by a constant and homogeneous surface buoyancy flux  $B_0$ , and

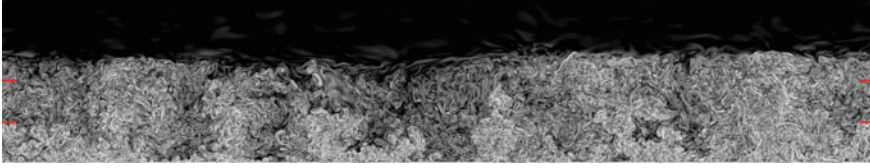


**Fig. 1** Vertical cross section of the logarithm of the enstrophy in the convective boundary layer. The horizontal bars at the side of the figures indicate a height equal to the CBL depth  $h$  and equal to half of it

the buoyancy stratification of the free atmosphere is  $N^2$ , where  $N$  is the buoyancy frequency. This configuration is representative of midday atmospheric conditions over land.

After the initial conditions have been sufficiently forgotten, statistical properties can be expressed as a function of the buoyancy Reynolds number  $Re_0 = B_0/(\nu N^2)$ , the normalized vertical distance to the surface  $z/h$ , and the normalized time  $tN$ . The variable  $h(t)$  is defined as  $h \simeq (2B_0N^{-2}t)^{1/2}$  and provides a measure of the CBL depth. The parameter  $L_0 = (B_0/N^3)^{1/2}$  is the reference Ozmidov scale and provides a measure of the thickness of transition layer at the top of the entrainment zone between the turbulent boundary layer and the free atmosphere. The ratio  $h/L_0$  increases as the CBL grows into the linearly stratified atmosphere. Beyond  $h/L_0 \simeq 10 - 15$ , the CBL is in a quasi-steady regime.

We consider data from a simulation with a buoyancy Reynolds number  $Re_0 = 117$  and at a state of development  $h/L_0 \simeq 21.5$ . The number of grid points used in the simulation are  $5120 \times 5120 \times 1024$ , in the streamwise, spanwise and vertical directions, respectively. Further details can be found in [5]. For the analysis presented here we use five horizontal planes, namely,  $z \in \{0.29h, 0.43h, 0.71h, 1.0h, 1.14h\}$ .

## 4 Results

We first analysed one-dimensional spectra of different velocity components to check whether the K41 hypothesis is satisfied with a good accuracy in the considered flow case. We found that the inertial range scaling  $\sim k_1^{-5/3}$  can be best recognised for the longitudinal spectra of horizontal velocity components  $u$  and  $v$  and for the transverse spectra of the vertical velocity component  $w$ . In this latter case, however, the proportionality constant again exceeds the isotropic value  $\alpha' = 0.65$ . Deviations from the K41 scaling were observed for the transverse spectra of  $u$  and  $v$ , where  $\sim k_1^{-a}$  or  $\sim k_1^{-b}$  scaling, with  $a$  and  $b$  smaller than  $5/3$ , was found. Similar observations were reported in [1] in the case of stratocumulus cloud in the core, buoyancy-driven section of the cloud. This allows us to conclude that the deviations from K41 theory follow from the anisotropy of the flow due to buoyancy. As we expect, the EDR estimates based on atmospheric measurements may also be biased due to these effects, similarly as results presented in this paper.

**Table 1** Values of EDR calculated at horizontal plane  $z = 1.0h$ , where  $\epsilon_{DNS}/B_0 = 0.26$ . The first fitting ranges seemed optimal for power spectra, the second—for structure functions

|            | $\frac{\epsilon_{SR}}{B_0}$ | $\Lambda/\lambda_n$ | $\frac{\epsilon_\lambda}{B_0}$ | $k$ -fitting range | $\frac{\epsilon_{PS}}{B_0}$ | $\frac{\epsilon_{NC}}{B_0}$ | $k$ -fitting range | $\frac{\epsilon_{PS}}{B_0}$ | $\frac{\epsilon_{NC}}{B_0}$ | $\frac{\epsilon_{D_2}}{B_0}$ | $\frac{\epsilon_{D_3}}{B_0}$ |
|------------|-----------------------------|---------------------|--------------------------------|--------------------|-----------------------------|-----------------------------|--------------------|-----------------------------|-----------------------------|------------------------------|------------------------------|
| $u$ in $x$ | 0.16                        | 1.21                | 0.24                           | 38–71              | 0.28                        | 0.24                        | 12–20              | 0.22                        | 1.2                         | 0.18                         | 0.10                         |
| $v$ in $y$ | 0.18                        | 1.16                | 0.24                           | 38–71              | 0.28                        | 0.22                        | 12–20              | 0.22                        | 1.2                         | 0.18                         | 0.09                         |
| $u$ in $y$ | 0.14                        | 1.27                | 0.24                           | 63–126             | 0.30                        | 0.20                        | 20–33              | 0.18                        | 0.9                         | 0.16                         |                              |
| $v$ in $x$ | 0.16                        | 1.20                | 0.24                           | 63–126             | 0.30                        | 0.26                        | 20–30              | 0.18                        | 1.2                         | 0.16                         |                              |
| $w$ in $x$ | 0.18                        | 1.18                | 0.26                           | 10–20              | 0.30                        | 0.34                        | 12–20              | 0.32                        |                             | 0.22                         |                              |
| $w$ in $y$ | 0.18                        | 1.16                | 0.26                           | 10–20              | 0.34                        | 0.32                        | 12–20              | 0.32                        |                             | 0.22                         |                              |

**Fig. 2** EDR estimates of free convective boundary layer simulation calculated from (1)–(4) as a function of vertical coordinate. Fitting ranges were estimated based on  $D_2$ .  $\epsilon_{DNS}$  denotes the exact, DNS value of EDR

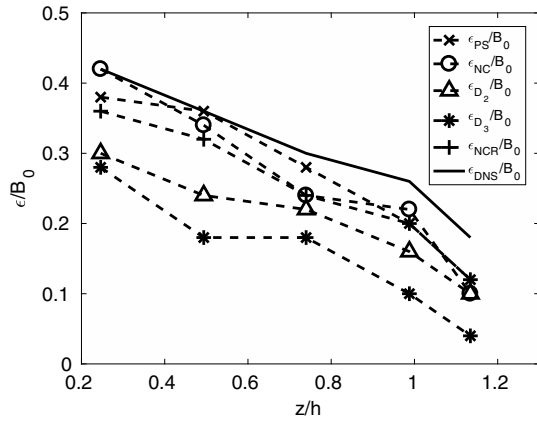


Table 1 presents values of  $\epsilon$  calculated using different EDR retrieval techniques described in Sect. 2 at horizontal plane  $z = 1.0h$ . Results were averaged in the homogeneous directions  $x$  or  $y$ . We observe a large deviation from unity of the  $\Lambda/\lambda_n$  ratio, which could be caused by strong non-Gaussianity of velocity derivatives or low- $Re$  effects. As a result,  $\epsilon_{SR}$  are underestimated. We found  $\epsilon_{PS}$  strongly depends on the chosen range of  $k$  values where the line  $k_1^{-5/3}$  is fitted. The same is true for other estimates. The first fitting range in Table 1 seemed to be optimal for the power spectra, the second—for the structure functions. Moreover, we observe that estimates from the vertical velocity component  $w$  differ from the remaining estimates.

Results of EDR estimates with different methods, averaged over horizontal signals ( $u$  in  $x$ ,  $v$  in  $y$ ,  $u$  in  $y$ ,  $v$  in  $x$ ) are presented in Fig. 2. We took fitting ranges that result form  $D_2$  function. As it is seen,  $\epsilon_{D_3}$  and  $\epsilon_{D_2}$ , which are standard method of  $\epsilon$  retrieval, are much underpredicted as compared to  $\epsilon_{DNS}$ . To calculate  $\epsilon_{NC}$  and  $\epsilon_{NCR}$  the DNS signal was first low-pass filtered with the use of the 6th order Butterworth filter (Matlab software). In case of  $\epsilon_{NCR}$ , the cut-off wavenumber  $k_{cut}$  was placed in the inertial range, see (4) and (5), and we used the Pope’s model for  $f_\eta$  [6]. We found, the  $\Lambda/\lambda_n$  ratio changes with cut-off wavenumber and is closer to 1 in the inertial

range, hence  $\epsilon_{\text{NC}}$  and  $\epsilon_{\text{NCR}}$  compare better with  $\epsilon_{\text{DNS}}$  than  $\epsilon_{\text{SR}}$ . In order to estimate  $\epsilon_{\text{NCR}}$  we apply the iterative procedure shortly summarised in Sect. 2. Independently of the initial guess of  $\eta^0$  the procedure always converged to the same value of  $\epsilon_{\text{NCR}}$  before the 10th iteration for  $d_\eta = 10^{-8}$ .

## 5 Conclusions

In this work, we investigated different EDR retrieval techniques on DNS data of convective boundary layer. Although the high  $Re$  numbers observed in nature could not be reached in the DNS, we can still test model assumptions and draw conclusions applicable also to “real-world” flows. We observed flow anisotropy due to buoyancy and, similarly as in [1], we found that estimates from horizontal velocity components compare better with  $\epsilon_{\text{DNS}}$ . We showed that estimates from number of crossing method proposed in [8] compare very well with  $\epsilon_{\text{DNS}}$ . In the considered flow case, the largest discrepancies were observed for estimates based on structure functions.

A perspective for a further study is to test performance of the EDR retrieval techniques on a larger set of experimental data of atmospheric flows.

**Acknowledgements** This work received funding from the European Union Horizon 2020 Research and Innovation Programme under the Marie Skłodowska-Curie Actions, Grant Agreement No. 675675. MW and SPM acknowledge matching fund from the Polish Ministry of Science and Higher Education No. 341832/PnH/2016.

## References

1. E.O. Akinlabi, M. Waclawczyk, J.P. Mellado, S.P. Malinowski, Estimating turbulence kinetic energy dissipation rates in numerically simulated stratocumulus cloud-top mixing layer: evaluation of different methods. *J. Atmos. Sci.* **76**, 1471–1488 (2019). <https://doi.org/10.1175/JAS-D-18-0146.1>
2. J.M. Kopeć, D. Kwiatkowski, S. de Haan, S.P. Malinowski, Retrieving atmospheric turbulence information from regular commercial aircraft using MODE-S and ADS-B. *Atmos. Meas. Tech.* **9**, 225–2265 (2016). <https://doi.org/10.5194/amt-9-2253-2016>
3. A.N. Kolmogorov, Dissipation of energy in locally isotropic turbulence. *Dokl. Akad. Nauk SSSR* **434**, 15–17 (1941)
4. S.P. Malinowski et al., Physics of stratocumulus top (POST): turbulent mixing across capping inversion. *Atmos. Chem. Phys.* **13**, 12 171–12 186. <https://doi.org/10.5194/587acp-13-12171-2013>
5. J.P. Mellado, C.C. van Heerwaarden, J.R. Garcia, Near-surface effects of free atmosphere stratification in free convection. *Bound.-Layer Meteorol.* **159**, 69–95 (2016)
6. S.B. Pope, *Turbulent Flows* (Cambridge University Press, Cambridge, 2000)
7. K. Sreenivasan, A. Prabhu, R. Narasimha, Zero-crossings in turbulent signals. *J. Fluid Mech.* **137**, 251–272 (1983). <https://doi.org/10.5194/amt-9-2253-2016>
8. M. Waclawczyk, Y.-F. Ma, J.M. Kopeć, S.P. Malinowski, Novel approaches to estimating turbulent kinetic energy dissipation rate from low and moderate resolution velocity fluctuation time series. *Atmos. Meas. Tech.* **10**, 4573–4585 (2017). <https://doi.org/10.5194/amt-10-4573-2017>